

Optimal Power Flow Scheduling Strategy for Multi-Microgrids with Multi-Time Scale Method

Panbao Wang^{*}, Yang Zhou, Xiaochen Zhang, Wei Wang and Dianguo Xu

Department of Electrical Engineering, Harbin Institute of Technology, Harbin, China

Abstract: The energy management of a multi-microgrid (MG) system is essential for its stable and economic operation. This study proposes an optimal power flow scheduling strategy for the energy management of multi-MG systems. At the multi-MG level, the global central controller (GCC) is responsible for managing the MGs. The GCC calculates the amount of power exchanged within the MGs by using a novel optimal energy allocation policy. Based on the energy supply and demand mismatch, MGs are classified as providers and consumers. The GCC collects information, then distributes energy among the consumers and divides benefits to the providers. Each consumer determines the price of the purchased energy from other microgrids based on a priority parameter, in which the local load demand and renewable energy penetration rate are considered as important factors. At the MG level, with the goal of minimising the operating cost of the MG, the energy is controlled from two time scales, namely day-ahead and intraday, to optimise the output power of generators and energy storage devices. Finally, a simulation of a multi-MG system with three MGs demonstrate the effectiveness of the proposed optimal method.

Keywords: Multi-microgrid, Multi-time scale, Power flow scheduling, Energy management, Renewable energy.

1. INTRODUCTION

As the energy demand and environmental issues increase worldwide, a large amount of renewable energy is flooding into the electricity market. To meet the challenges brought by the random and intermittent renewable energy generations (REGs) to the main grid, multi-microgrids (MGs) emerge as one of the promising solutions to integrate the REGs effectively [1-6]. MGs usually consist of distributed generations, loads, energy storage systems, etc. They can solve the connection problem between the REGs and the main grid by integrating coordinated control and energy management systems [7]. Generally, a single MG has a limited capability to maintain a stable and economic operation, while a combination of MGs, *i.e.* a multi-MG system, guarantees an improved ability. Compared with a single MG, multi-MG systems can ensure normal operation of the internal single MGs and can simultaneously balance the energy flows among the MGs in the system to improve the power quality and reliability, and reduce the distribution power losses [8-12]. Therefore, the coordinated operation control of multi-MGs is essential to realise an autonomous operation of the system.

From the decision-making point of view, two main approaches can be adopted for the control scheme of multi-MGs, *i.e.* decentralised control and centralized control methods [13]. In the decentralised approach, a

multi-agent system is employed, where each MG needs to follow a unified agreement. The main challenge of the decentralised control is how to establish a consensus among different agents in the MGs. In the centralised approach, the central controller provides the global optimised control strategy and conveys it to each MG. In [14], the centralised control method is used to achieve optimal energy trading results by using stochastic distribution functions to simulate energy uncertainty, and the influence of error on the scheduling results is considered. In [15, 16], the units in multi-MGs are classified into consumers and providers. Moreover, the energy trading among the MGs is described as a game problem, and each MG obtains its optimal operation results during the game. In [17], a contribution-based energy-trading mechanism among MGs in a competitive market is proposed and is described as a non-cooperative energy competition game. In [18], a power scheduling method-based priority is proposed. The priority value of the MG is determined by its previous contribution value, and the energy trading among the MGs is determined according to this priority. In [19], hunger parameters are introduced for the energy allocation in multi-MGs. In [20], a two-stage optimisation model based on a dynamic electricity pricing strategy, which can smooth the load curve of the main grid as well as reduce the total operation cost of the MGs, is proposed.

Furthermore, aiming at managing multi-MGs more efficiently, the prediction of REGs and loads is another primary problem. A higher prediction accuracy will be more useful for an efficient power control of multi-MGs. At present, unsolved problems in the power forecast of

^{*}Address correspondence to this author at the Department of Electrical Engineering, Harbin Institute of Technology, Harbin, China; Tel: +8645186403020; E-mail: wangpanbao@hit.edu.cn

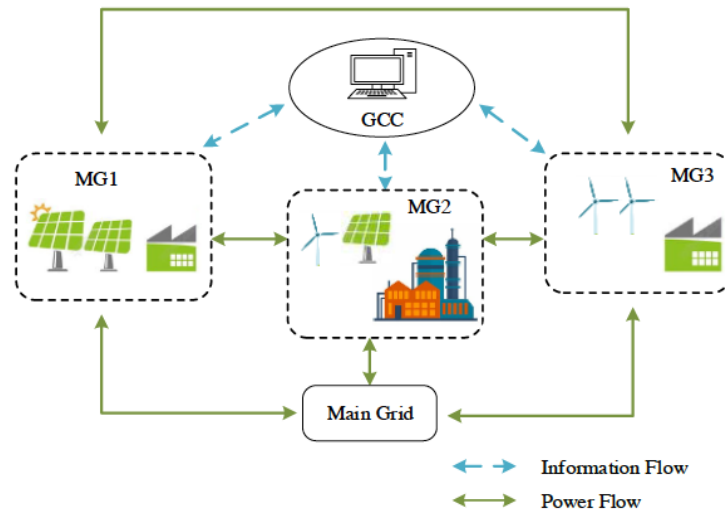


Figure 1: Structure of a multi-MG system.

REGs and loads still exist [21-23], and relying only on the day-ahead forecast is not enough. According to the characteristic that the prediction accuracy of renewable energy power increases with a decreasing time scale, increasing the prediction frequency of REGs and correcting the optimal scheduling scheme are effective methods for eliminating the impact of the random and intermittent problems of REGs. A multi-time scale power control method presented in [24] with three time scales is proposed to stabilise the power fluctuation, wherein the effectiveness of the proposed power control method is verified by real-time hardware-in-loop tests. In addition, a bilayer multi-time coordination method is proposed in [25]. In the day-ahead schedule layer, generating units are committed, and relaxed bidirectional reserve boundaries are predicted for the next day. In the real-time dispatch layer, the generation output is dynamically adjusted and the reserve is dispatched using successive approximations based on real-time data.

As can be found from the existing studies of multi-MGs, the prediction errors of REGs during the energy management of multi-MGs should be taken into consideration. However, if these errors cannot be calculated and processed correctly, they will have a very negative impact on the operation of multi-MGs. In order to fill the above-mentioned gaps, this study establishes a centralised control strategy based on a multi-time scale for the energy management of multi-MGs. In addition, this study proposes an energy trading method based on a proportional distribution to solve the problem of energy trading among different MGs. The main contributions of this study are as follows:

1) Proposing a novel method for calculating the priority parameter (PP) of MGs with consideration of the penetration rate of REGs and energy demand.

2) Applying a multiple time scale strategy to multi-MGs for reducing the negative effects of REGs forecasting errors.

The rest of this paper is organised as follows. In Section 2, the energy management framework of multi-MGs adopted in this study is presented. Section 3 introduces the proposed optimal power flow scheduling strategy of multi-MGs. Section 4 discusses the corresponding case studies conducted and evaluated. Finally, Section 5 provides the conclusion.

2. ENERGY MANAGEMENT FRAMEWORK OF MULTI-MGS

Geographically proximate MGs can be connected to form a multi-MG system. In this system, each MG has the benefit of acquiring power from neighbouring MGs in case of insufficient power, or providing power to other MGs when extra power is available. Additionally, if there is still excess or insufficient power in the system, it can exchange energy with the main grid. As shown in Figure 1, by interconnecting the MGs with power lines and two-way communication lines, a multi-MG system is established.

This study adopts a hierarchical control system [26-29] to accomplish an efficient energy trading between multi-MGs. As shown in Figure 2, using the hierarchical control efficiently reduces the logic complexity and completes the energy scheduling through different levels of coordination. First, at the multi-MG level, a global central controller (GCC) is responsible for

coordinating the operation of MGs. With the power scheduling execution at this level, the GCC calculates the energy trading values between MGs and transmits commands to the MG central controllers (MCCs). At the MG level, a decision-making approach based on the multi-time scale energy scheduling strategy is adopted for the local operation management.

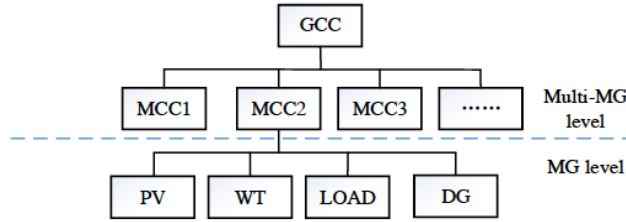


Figure 2: Hierarchical control for multi-MGs.

As mentioned previously, the effectiveness of the hierarchical control is closely related to the predictive correctness of REGs. To reduce the negative effects of prediction errors of the control method, a multi-time scale energy scheduling, which includes two stages [30, 31], *i.e.* day-ahead and intraday, is employed. In the day-ahead scheduling period, according to the day-ahead forecast of REGs and loads, the GCC calculates the optimal energy trading among MGs per hour on the next day. Based on the energy trading plan formulated by the GCC, the MCCs calculate the output of the diesel generator, the charge and discharge power of the battery, and the power exchanged with the main grid per hour on the next day. In this period, the technical characteristics of the output units, energy storage state, time-of-use electricity price, and fuel price of the batteries are considered to obtain the lowest daily operating cost of the MG. In the intraday period, the intraday forecast information is scrolled and updated in a cycle of 15 min. Based on the results of the day-ahead scheduling including energy trading among the MGs and the power exchanged with the main grid, the MCCs optimise the output of the diesel generators and batteries, trying to eliminate the deviation caused by the day-ahead forecast error, and ensure a stable operation.

3. PROPOSED OPTIMAL POWER FLOW SCHEDULING STRATEGY

3.1. Energy Allocation Policy Among MGs in Multi-MG Level

In the proposed multi-MG system, it is assumed that there are m MGs. $M = \{MG_1, MG_2, MG_3, \dots, MG_m\}$ represents the collection of all MGs in this system.

Within a certain time t , the difference between the renewable energy and the load power generated by the i -th MG can be defined as a net energy value, and it can be calculated as

$$\Delta P_i^t = P_{PV_i}^t + P_{wti}^t - P_{loadi}^t \quad (1)$$

where $P_{PV_i}^t$, P_{wti}^t , and P_{loadi}^t are the estimated values of the photovoltaic and wind turbine generation, and the local consumption of the i -th MG at time t , respectively. If $\Delta P_i^t < 0$, MG i is regarded as a consumer; otherwise, it is considered as a provider. During this period t , the provider delivers energy to the consumers, and the energy flow will be within the multi-MG system, avoiding frequent energy exchange between the multi-MG system and the main grid. In addition, the price of the traded energy among MGs is lower than the price of electricity purchased from the main grid, and is higher than the price of electricity sold to the main grid. Through the energy trading process, the overall benefits of the multi-MG system are improved. In the process of energy trading, allocating energy to consumers and maximising the benefits to providers as well as ensuring the fairness of the trading market are critical issues.

To solve the aforementioned problems, this study proposes a new method for energy trading among MGs. The supplementary energy offered by the providers is allocated to the consumers in proportion to the bid of consumers, and the revenue is distributed to the providers in proportion to the sales. The bid of consumer i is based on the value of the PP, which is determined by two factors:

1. The energy demanded by the i -th consumer, where more energy demand results in a higher bid;
2. The renewable energy penetration rate of the MGs. To encourage MGs that are developing clean energy and promoting energy transformations, consumers with a high penetration rate can obtain the energy preferentially.

Therefore, the PP in the present interval can be calculated as

$$PP^t = \alpha_i \frac{L_i^t}{L_{Total}^t} + \beta_i u_i^t \quad (2)$$

$$u_i = \frac{\sum_{t=1}^{24} (P_{wti}^t + P_{pvi}^t)}{\sum_{t=1}^{24} P_{loadi}^t} \quad (3)$$

$$C_i^t = PP(C_{GS}^t - C_{GB}^t) + C_{GB}^t \quad (4)$$

In (2), L_i is the load demand of consumer i , and L_{Total} is the total demand from all consumers. α_i and β_i are the weight factors ($0 \leq \alpha_i, \beta_i \leq 1$, and $\alpha_i + \beta_i = 1$). C_i^t is the bid of the i -th consumer, C_{GS}^t is the price of electricity purchased from the main grid, and C_{GB}^t is the price of electricity sold to the main grid. From (2)–(4), it can be observed that $C_{GB}^t < C_i^t < C_{GS}^t$, which can enable energy trading among MGs preferentially and then exchange energy with the main grid.

At time t , the energy that the i -th consumer obtains from energy trading can be expressed as

$$B_i^t = \begin{cases} -\Delta P_i^t, & 0 < E_b^t \leq E_s^t \text{ or } E_b^t > E_s^t > 0 \text{ and } \sum_{i \in I} \frac{C_i^t}{C_i^t} E_s^t > \Delta P_i^t \\ \sum_{i \in I} \frac{C_i^t}{C_i^t} E_s^t, & E_b^t > E_s^t > 0 \text{ and } \sum_{i \in I} \frac{C_i^t}{C_i^t} E_s^t < \Delta P_i^t \\ 0, & \text{others} \end{cases} \quad (5)$$

where E_b^t is the sum of the energy required by all consumers during time t , and E_s^t is the sum of the energy supplied by all providers. If $E_b^t < E_s^t$, each consumer will get its required energy, and the remaining energy is sold to the main grid. If $E_b^t > E_s^t$, the total energy supplied by the providers is allocated to the consumers in a proportion based on the bid of consumers and it does not exceed the energy required by the consumers.

The actual energy supplied by provider j is mainly dependent on the renewable energy penetration rate, which can be derived as

$$u_j = \frac{\sum_{t=1}^{24} (P_{wjt}^t + P_{pvj}^t)}{\sum_{t=1}^{24} P_{loadj}^t} \quad (6)$$

where u_j is the renewable energy penetration rate of provider j . Compared with selling to the main grid, providers with high renewable energy penetration rates can get more revenue by selling energy to other MGs. Similar to the calculation method of consumer bid, the purpose of this approach is to allow the MGs to develop more renewable energy for profit.

At time t , the energy that the j -th provider can deliver in the process of energy trading can be expressed as

$$S_j^t = \begin{cases} \Delta P_j^t, & E_b^t > E_s^t > 0 \text{ or } E_s^t > E_b^t > 0 \text{ and } \sum_{j \in J} \frac{u_j}{u_j} E_b^t > \Delta P_j^t \\ \sum_{j \in J} \frac{u_j}{u_j} E_b^t, & E_s^t > E_b^t > 0 \text{ and } \sum_{j \in J} \frac{u_j}{u_j} E_b^t < \Delta P_j^t \\ 0, & \text{others} \end{cases} \quad (7)$$

If $E_b^t < E_s^t$, the provider outputs the energy proportionally according to the renewable energy penetration. If $E_b^t > E_s^t$, each provider outputs the total excess energy.

The total revenue from all providers of the multi-MGs in the process of energy trading is given as

$$R^t = \sum_{i \in I} B_i^t C_i^t \quad (8)$$

Meanwhile, the revenue of the j -th provider can be derived as

$$R_j^t = \frac{S_j^t}{\sum_{j \in J} S_j^t} R^t \quad (9)$$

Based on the above analysis and description, the flow chart of the proposed energy trading process can be depicted as shown in Figure 3.

3.2. Multi-Time Scale-Based Energy Management in MG Level

The energy management of MGs is able to calculate the power flows within the MG including the exchange of power from the main grid, the output power of each diesel generator, and the charging and discharging power of the energy storage devices. In this study, to eliminate deviations caused by forecast errors, different control strategies are adopted in different stages as follows.

3.2.1. Day-Ahead Power Scheduling

According to the day-ahead forecast information, while the minimum operating cost of the MG is considered as the optimisation objective, the MCCs optimise the output of different units in the MG. In the process, the time-of-use electricity price, battery operating life loss and operating cost, diesel generator

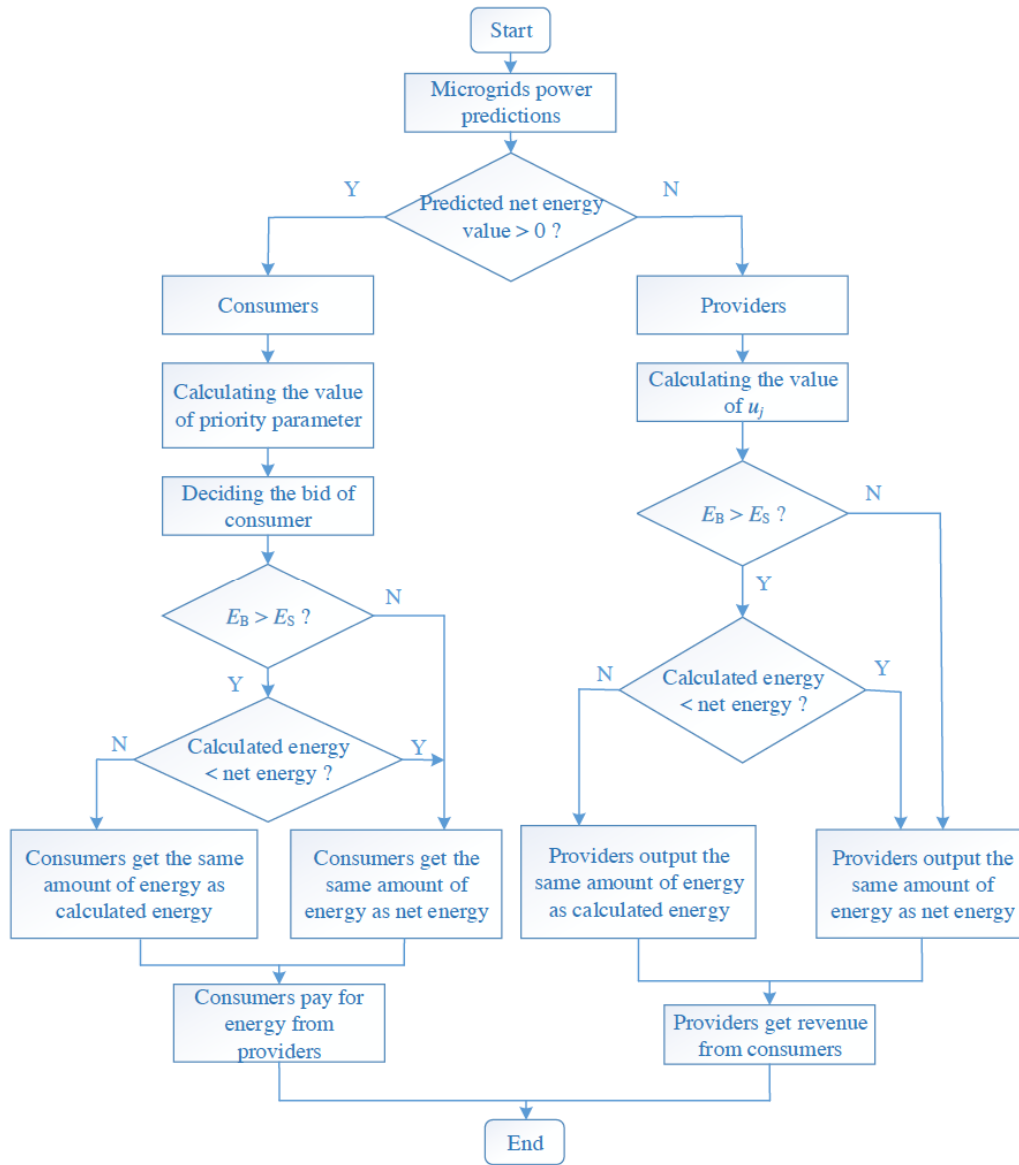


Figure 3: Flow chart of the proposed energy trading process.

operating cost, and the main grid power price, as well as the demand side management are considered.

The objective function to be minimised at each time step (t) can be expressed as follows:

$$\min F_1 = \min \sum_{t=1}^{24} \sum_{i=1}^m [C_{bat}(P_{bati}^t) + C_{grid}(P_{gridi}^t) + C_{de}(P_{dei}^t) + C_{load}(P_{loadi}^t)] \quad (10)$$

where $C_{bat}(P_{bati}^t)$ is the operation and maintenance cost of the battery in MG i during the time interval t , $C_{de}(P_{dei}^t)$ is the operation cost of the diesel generator in MG i during the time interval t , and $C_{grid}(P_{gridi}^t)$ is the cost of exchanging power with the main grid.

When modelling the load, by taking into account the demand side response, the loads that can participate in the optimisation are divided into two, *i.e.* interruptible load and moveable load. An interruptible load means that the MG can interrupt it at any time. If it is interrupted, it needs to be compensated accordingly. The characteristic of the moveable load is that there is a user's willingness to start and stop, and the start and stop time of the operation can be flexibly changed according to the actual situation and when the power level is constant.

$$C_{load}^t = u_{cut}^t P_{cut}^t d_{cut}^t + |u_s^t - u_{shift}^t| P_{shift}^t d_{shift}^t \quad (11)$$

where P_{cut}^t and P_{shift}^t correspond to the power plan

values of the interruptible and moveable loads, respectively; d_{cut}^t and d_{shift}^t are the electricity prices corresponding to the interruptible and moveable loads, respectively; u_{cut}^t is the optimised operating state of the interruptible load ($u_{cut}^t = 1$ when the load is removed or 0 if the load is connected); u_s^t and u_{shift}^t represent the willingness of users to run the state and the optimised running state, respectively (1 means that the load is running and 0 means it is not). When the operating status made by the users and the actual operating status are not equal, the user should be compensated accordingly.

The constraints, which are essential to meet the day-ahead optimising process, are presented as follows:

$$P_{pvi}^t + P_{wti}^t + P_{bati}^t + P_{dei}^t + P_{gridi}^t + \sum_{i \neq j} P_{i,j}^t = P_{loadi}^t \quad (12)$$

$$P_{gridi}^t \leq |P_{gridi}^{\max}| \quad (13)$$

$$P_{dei}^{\min} \leq P_{dei}^t \leq P_{dei}^{\max} \quad (14)$$

$$E_{bat}^t = E_{bat}^{t-1}(1-\sigma) - \Delta P / \eta_{dh} \quad (15)$$

$$E_{bat}^t = E_{bat}^{t-1}(1-\sigma) - \Delta P / \eta_{dh} \quad (16)$$

$$SoC_{\min} < SoC < SoC_{\max} \quad (17)$$

$$0 \leq P_{chi}^t \leq P_{chi}^{\max} \quad (18)$$

$$P_{dhi}^t \leq |P_{dhi}^{\max}| \quad (19)$$

where $P_{i,j}^t$ is the flowing power from MG i to MG j , and

P_{gridi}^{\max} is the maximum allowable power to be transmitted between MG i and the main grid. When MG i purchases electricity from the main grid, the power value is positive, and it is negative when the power is sold to the main grid; P_{dei}^{\min} and P_{dei}^{\max} are respectively the minimum and maximum limited power of the diesel generator in MG i . When the battery is charged, E_{bat}^t is the sum of the power of the previous moment and the charging power per unit time; when the battery is discharged, E_{bat}^t is the difference between the power of the previous moment and the discharge power per unit time; σ is the self-discharge coefficient of the battery; η_{ch} and η_{dh} are the charging and discharging efficiency of the battery, respectively; SoC is the state of charge of the battery during charging and discharging;

P_{chi}^{\max} and P_{dhi}^{\max} are the maximum charging and discharging power of the battery in MG i , respectively. The day-ahead power scheduling strategy is as follows.

Algorithm 1 Day-ahead power scheduling strategy

1. The MCCs calculate the day-ahead energy surplus/shortage of MGs based on the forecasted renewable energy production and consumer demand during the adopted optimisation period.
2. The MCCs send the predicted power balance information of MGs to the GCC.
3. The GCC determines energy trading among the MGs according to (2)–(8).
4. The GCC sends the energy trading results to the MCCs.
5. The MCCs develop an optimisation management plan based on the day-ahead prediction information to decide the exchange of power with the main grid.

3.2.2. Intraday Power Scheduling

In the intraday stage, the intraday prediction information of the REGs and loads is updated in a cycle of 15 min, and the rolling optimisation is conducted, including the charge and discharge power of each MG energy storage device and the output power of the diesel generator.

The intraday forecast period, time resolution, and control period are 4 h, 15 min, and 15 min, respectively. The intraday scheduling strategy mainly includes the following steps:

1) At time k , based on the prediction model, the MCCs predict the amount of power in the system within 4 h (16 periods) and consider the current and future constraints; then the MCCs solve the optimisation problem to obtain the power plan at time $k+1$, $k+2$, ..., $k+16$;

2) Only the $[k, k+1]$ period is controlled to carry out the plan scheduled at time k , and the results at time $k+1$ are output as the initial values of the $[k+1, k+2]$ period;

3) The above steps are repeated to make the plan at time $k+1$.

The intraday optimisation objective function of MG i can be expressed as

$$\min F_2^i = \min \sum_{k=1}^{96} \left[C_{bat} \left(P_{bati}^k \right) + C_{de} \left(P_{dei}^k \right) \right] \quad (20)$$

where $C_{bat} \left(P_{bati}^k \right)$ is the operation and maintenance cost of the battery in MG i during time t , and $C_{de} \left(P_{dei}^k \right)$ is the operation cost of the diesel generator in MG i during time t . The intraday power scheduling strategy is as follows.

Algorithm 2 Intraday power scheduling strategy

1. The MCCs forecast the intraday power of the REGs and load demand.
2. The MCCs determine the charge and discharge power of the energy storage device and the output power of the diesel generator based on the forecasted power and the results calculated in the day-ahead scheduling.

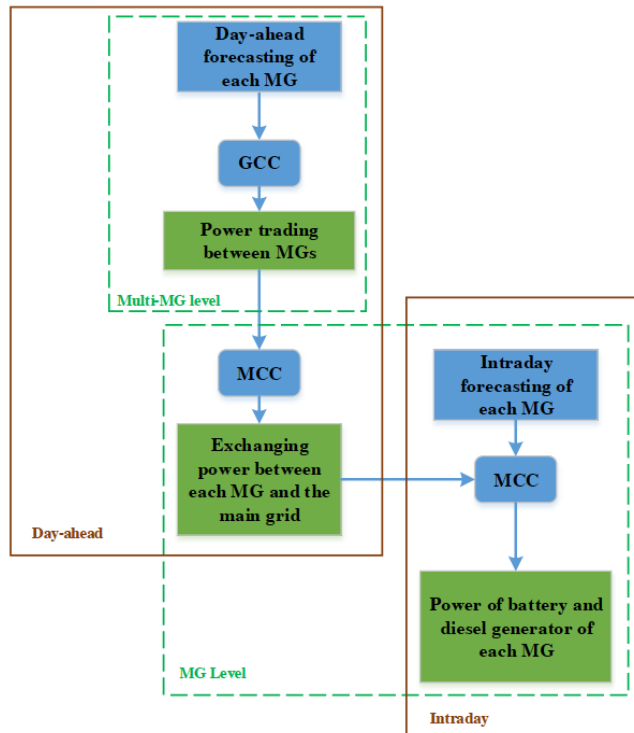


Figure 4: Diagram of the proposed optimal power flow scheduling strategy.

Table 1: Configuration of Multi-MGs

	Wind Installed Capacity (kW)	Photovoltaic Installed Capacity (kW)	Battery Capacity (kWh)	Diesel Generator Maximum Power (kW)	Load Type
MG 1	1080	875	2000	200	Industrial load
MG 2	571	403	1800	200	Resident load
MG 3	800	0	1200	100	Resident load

The constraints of the intraday scheduling are consistent with those of the day-ahead scheduling, and the optimal scheduling results can be obtained by the particle swarm optimisation (PSO) algorithm.

In summary, Figure 4 shows the whole strategy of the proposed optimal power flow scheduling for the multi-MG system, which reveals the relationship between different control levels and different time scales.

4. SIMULATION VERIFICATION AND CASE STUDIES

The effectiveness and performance of the proposed multi-time scale-based optimal power flow scheduling strategy for multi-MGs are validated and studied. In the simulation, three connected MGs constitute the multi-MG system. The detailed configuration parameters of each MG are presented in Table 1.

As indicated in Table 1, α_i and β_i of each MG are both 0.5, indicating that the renewable energy penetration rate and power difference have the same impact on the bidding of each MG. The initial SoC of the batteries in the MGs is set as 0.5, and the maximum and minimum limits are 0.9 and 0.2, respectively.

When a single MG exchanges energy with the main grid, a time-of-use electricity price is adopted. The specific purchase and sale prices are listed in Table 2. As can be observed, the peak hours are 11:00–15:00 and 19:00–21:00, and the average time is 08:00–10:00, 16:00–18:00, and 22:00–23:00. The valley time is 00:00–07:00.

Table 2: Time-of-Use Electricity Price

Project	Prices / (Yuan / kWh)		
	Peak hours	Average time	Valley time
Purchase	0.83	0.49	0.27
Sale	0.65	0.38	0.13

4.1. Multi-MG Level Simulation Results

The power allocations of different MGs are shown in Figure 5. The solid line in the figure denotes the predicted net energy value. Positive values of P_{ij} represent the transferred power from MG i to MG j , and negative values of P_{ij} represent the transmitted power from MG j to MG i . P_{ig} represents the power surplus or shortage of MG i after power allocations.

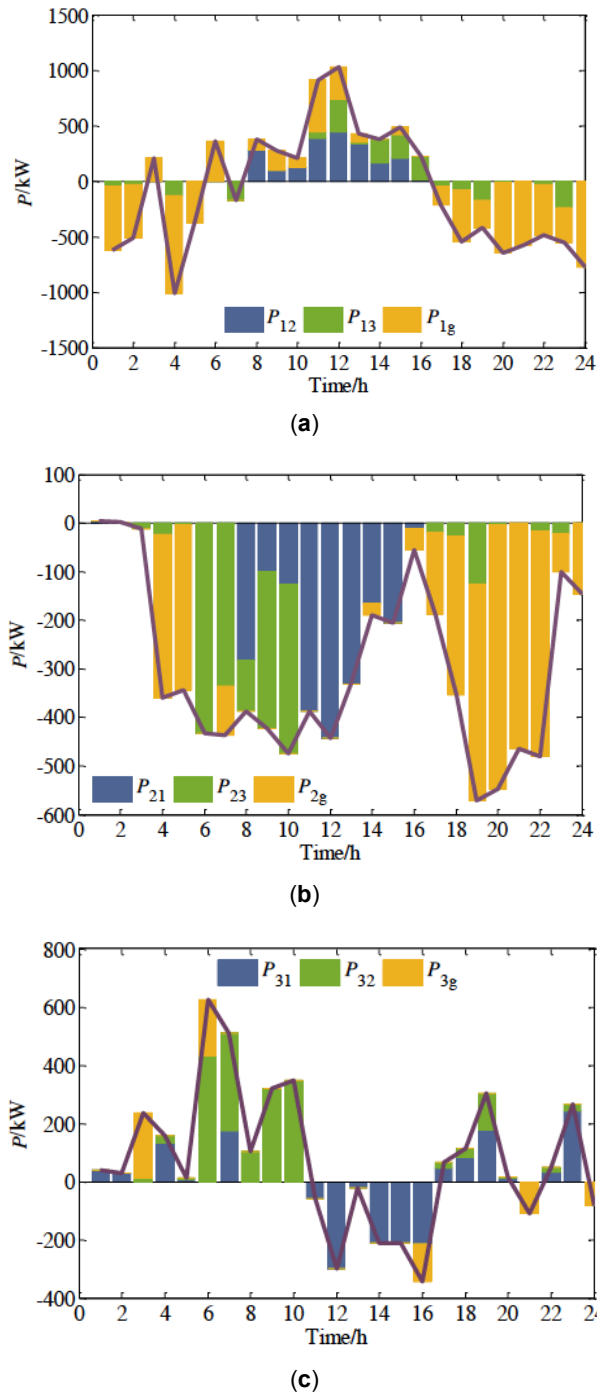


Figure 5: Predicted energy net value and power allocation references: (a) MG1, (b) MG2, and (c) MG3.

As can be observed in Figure 5, MG 1 transfers excess energy to the other two MGs during the period 7:00–16:00. In other periods, MG 1 and MG 2 suffer from power shortages, while MG 3 has a power surplus; therefore, MG 3 transfers energy to the other two MGs. By comparing the values of the solid line and the values of P_{ig} , it can be found that the energy allocation can reduce the power surplus or shortage of a single MG, and the energy is exchanged and consumed within the multi-MG system.

Figure 6 shows the economic costs of a multi-MG system in a single MG mode and multi-MG mode, respectively. The single MG mode means that the MG operates separately and does not trade energy with other MGs, whereas the multi-MG mode means that the three MGs can exchange energy at any time. From the proposed energy allocation method, for a single MG, the purchase price of electricity from an adjacent MG is lower than that purchased from a large grid. Meanwhile, the price of selling excess energy to an adjacent MG is higher than the price when selling to the main grid. The transactional energy between MGs can reduce the operating costs of each MG. It can be observed from Figure 6 that the economic costs generated by the operation in the multi-MG mode are lower than those of the single MG mode. Among them, the economic cost of MG 3 is negative, indicating that a profitable state is achieved due to the high power generation of renewable energy.

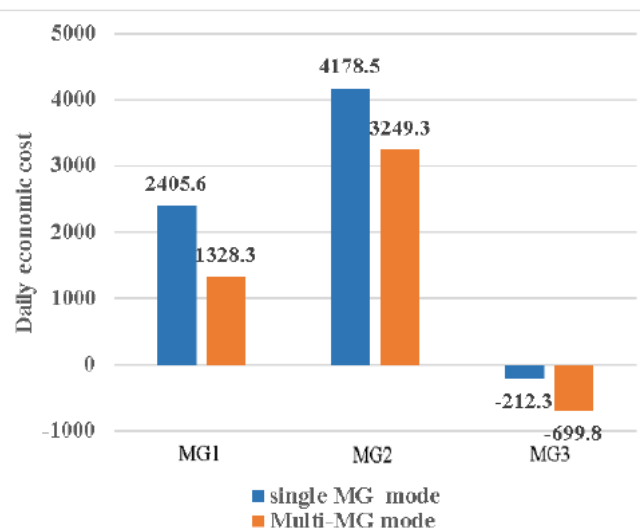


Figure 6: Daily economic cost of the three MGs.

4.2. MG Level Simulation Results

By taking MG 1 as an example, the optimal scheduling results of the single MG in a multi-MG

system are analysed. The load classification is indicated in Table 3. The power required by very important loads must be guaranteed to be continuously provided and is not involved in the load optimisation.

Table 3: Load Classification of MG1

Name	Capacity	Type
Load1	200kW	Very important
Load2	100kW	Moveable
Load3	150kW	Moveable
Load4	150kW	Very important
Load5	180kW	Very important
Load6	220kW	Very important
Load7	150kW	Interruptible
Load8	100kW	Interruptible
Load9	50kW	Moveable
Load10	100kW	Moveable

The PSO algorithm is used to calculate the objective function of the day-ahead stage. A typical load forecast curve is shown in Figure 7. The optimised load state is shown in Figure 8. The output curves of the power generation units and the SoC of the energy storage are shown in Figures 9 and 10, respectively.

As can be observed from Figure 8, the load change amplitude after optimisation adjustment is reduced. The moveable load during the peak time of electricity price is transferred to the valley time and average time. The interruptible load during the peak time is cut off. Load optimisation not only alleviates the pressure of the main grid to transmit a large amount of power during the peak time, but also reduces the economic cost of MG 1. It can be observed from Figure 9 that after load optimisation, the SoC curve of the energy storage is more gradual, and the depth of charge and discharge is lower, which can prolong its service life and achieve better economic benefits.

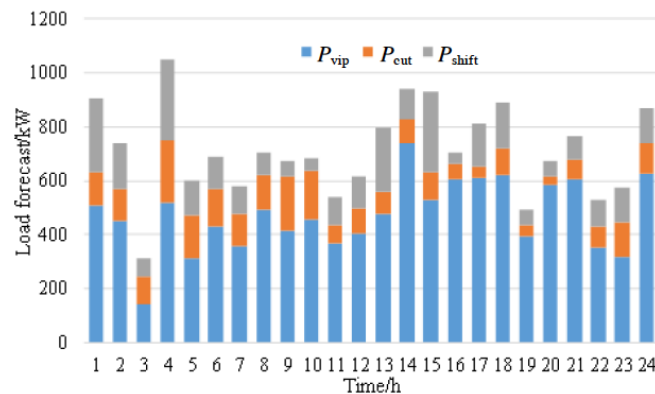


Figure 7: Load forecast data of MG 1.

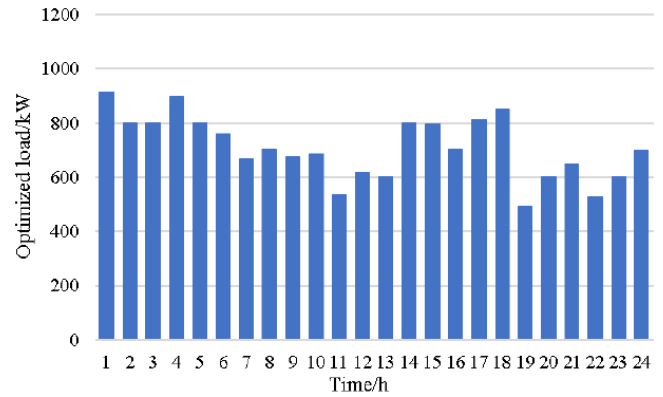


Figure 8: Optimised load data.

During the valley time (*i.e.* 0:00–7:00), as shown in Figure 10, MG 1 mainly purchases electricity from the main grid. The energy storage device is charged at this stage to benefit from the rational use of energy storage. During the electricity peak time (*i.e.* 19:00–21:00), MG 1 sells electricity to the main grid. At this time, the diesel generator fully generates electricity and the battery is charged to meet the load demand. The battery is mainly charged during electricity price valley time or the time when the load demand is less, and discharged during the peak time of the electricity price or the time when load demand becomes high. As a result, the function of ‘shaving the peak and filling the valley’ is realised and the economics of the system is improved.

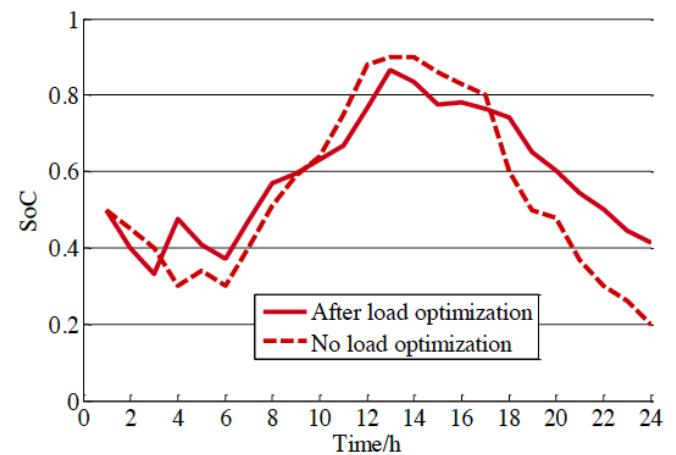


Figure 9: Comparison of SoC of energy storage devices.

In this study, we assumed that the error of renewable energy and load forecasting in the day-ahead stage is within 20%, and the cycle is optimised for 96 times in the period of 15 min. Compared with the day-ahead prediction power accuracy, the intraday prediction accuracy is significantly improved.

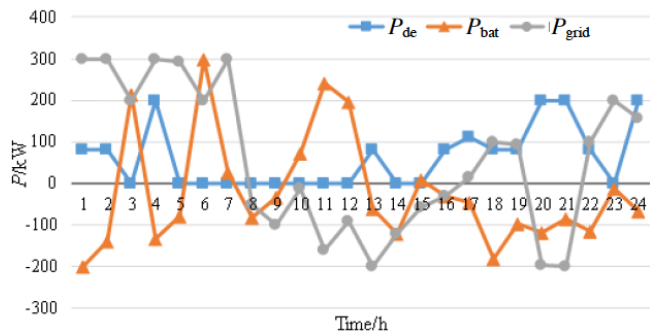


Figure 10: Power references of different units in MG 1.

As shown in Figure 11, the day-ahead predicted error is corrected by the battery and the diesel generator in the intraday stage, while the power exchanged with the main grid remains unchanged. Compared with the power reference of the battery in day-ahead, the output of the battery in intraday is not much different. Relative to the battery output change value, that of the diesel generator changes a lot. It can be observed from Figure 12 that the diesel generator plays a major role in correcting the dispatching reference of the day-ahead to avoid short-term charging and discharging of the batteries, which affect their service lives. Therefore, as shown in Figure 13, the SoC of the energy storage is able to follow the reference value of the day-ahead.

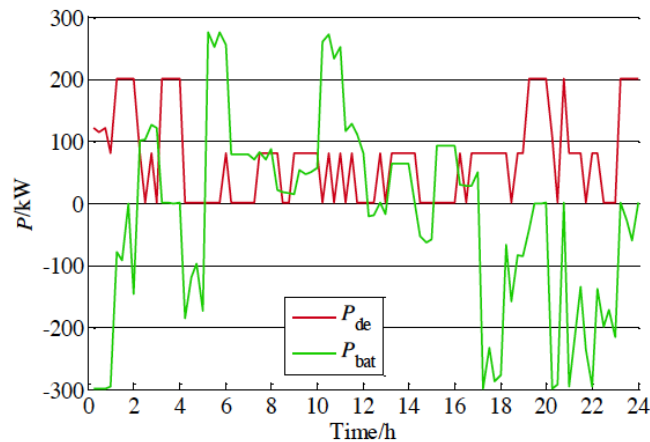


Figure 11: Outputs of MG 1 in intraday stage.

Figure 14 shows the comparison results of power exchanged with the main grid of the multi-MG system. As can be observed, when the intraday rolling optimisation is deactivated, the power exchanged with the main grid fluctuates basically near the day-ahead reference value, and it is difficult to realise a smooth and controllable scheduling of the MGs with the main grid. After the intraday rolling optimisation scheduling is activated, the exchange of power with the main grid

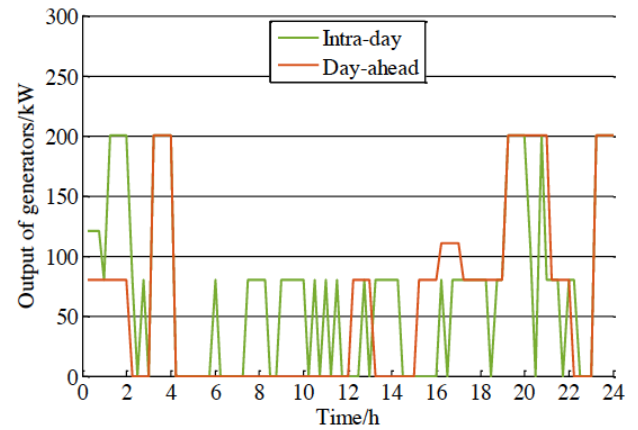


Figure 12: Comparison of output of diesel generators in the two stages.

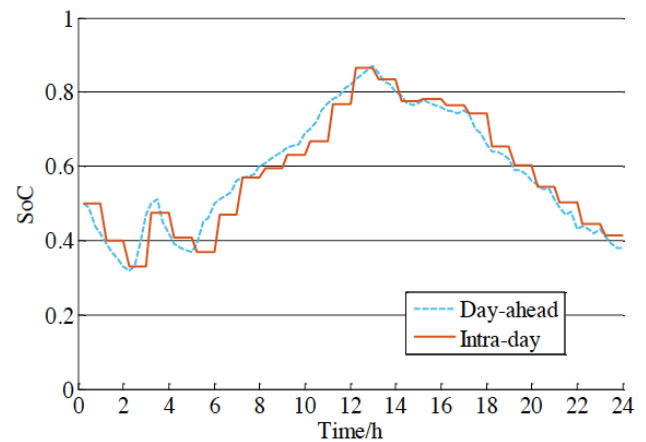


Figure 13: Comparison of SoC of energy storage devices in the two stages

can be kept constant from the power reference in the day-ahead, and the outputs of the battery and diesel generator can be adjusted to eliminate the actual planned deviation due to the forecast error in the day-ahead stage.

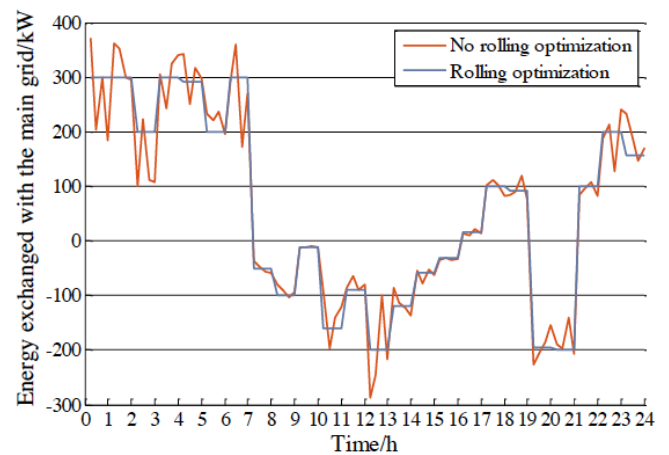


Figure 14: Comparison of power exchanged with the main grid.

5. CONCLUSION

The multi-MG system adopted in this study consists of three MGs, and each MG is managed by the GCC and connected to each other through power lines. A multi-time scale-based optimal power flow scheduling strategy is proposed to obtain a stable and economic operation of multi-MGs. Primarily, the energy allocation method ensures an optimal allocation of energy to the consumers based on the local load demand and the penetration rate of renewable energy sources. The extra energy is absorbed within the multi-MG system preferentially, which improves the economic benefits of the system. Furthermore, this study employs a multi-time scale method to reduce the optimisation error. The exchange of power between each MG and the main grid is given at the day-ahead stage, and the intraday scheduling uses the partial day-ahead results, which shortens the calculation time of the intraday scheduling and can meet the practical application requirements of the energy management strategy. After presenting the proposed energy allocation policy and day-ahead and intraday power scheduling, simulation studies and comparison analysis are conducted. It is shown that significant cost reductions and an improved operation of the multi-MG system are achieved.

ACKNOWLEDGMENT

This work was supported in part by the National Natural Science Foundation of China under Grant 51707045 and in part by the Postdoctoral Science Foundation of Heilongjiang Province of China under Grant LBH-Z17062 and in part by the Fundamental Research Funds for the Central Universities under Grant HIT.NSRIF.2019023.

REFERENCES

- [1] J.M. Guerrero, P.C. Loh, T. Lee and M. Chandorkar, "Advanced Control Architectures for Intelligent Microgrids-Part II: Power Quality, Energy Storage, and AC/DC Microgrids," *IEEE Transactions on Industrial Electronics*, 2013; 60(4): 1263-1270.
<https://doi.org/10.1109/TIE.2012.2196889>
- [2] A. Rasoolzadeh and F. R. Salmasi, "Reduced-order dynamic model for droop-controlled inverter/converter-based low-voltage hybrid AC/DC microgrids - part 1: AC sub-microgrid," *IET Smart Grid*, 2018; 1(4): 123-133.
<https://doi.org/10.1049/iet-stg.2018.0069>
- [3] T. Dragičević, X. Lu, J. C. Vasquez, *et al.*, "DC Microgrids-Part I: A Review of Control Strategies and Stabilization Techniques," *IEEE Transactions on Power Electronics*, 2016; 31(7): 4876-4891.
- [4] T. Dragičević, X. Lu, J. C. Vasquez, *et al.*, "DC Microgrids-Part II: A Review of Power Architectures, Applications, and Standardization Issues," *IEEE Transactions on Power Electronics*, 2016; 31(5): 3528-3549.
<https://doi.org/10.1109/TPEL.2015.2464277>
- [5] Giel Van den Broeck, Jeroen Stuyts, Johan Driesen, "A critical review of power quality standards and definitions applied to DC microgrids," *Applied Energy*, 2018; 31: 281-288.
<https://doi.org/10.1016/j.apenergy.2018.07.058>
- [6] Jiancheng Yu, Chris Marnay, Ming Jin, *et al.*, "Review of Microgrid Development in the United States and China and Lessons Learned for China," *Energy Procedia*, 2018; 145: 217-222.
<https://doi.org/10.1016/j.egypro.2018.04.038>
- [7] Xingyou Zhang, Bo Chen, Yan Cheng, *et al.*, "A Multi-microgrids System Model Considering Stochastic Correlations Among Microgrids," *Energy Procedia*, 2018; 145: 3-8.
<https://doi.org/10.1016/j.egypro.2018.04.002>
- [8] Jun-Sung Kim, Seong Min So, Joong-Tae Kim, *et al.*, "Microgrids platform: A design and implementation of common platform for seamless microgrids operation," *Electric Power Systems Research*, 2019; 167: 21-38.
<https://doi.org/10.1016/j.eprsr.2018.10.019>
- [9] Z. Xu, P. Yang, Y. Zhang, *et al.*, "Control devices development of multi-microgrids based on hierarchical structure," *IET Generation, Transmission & Distribution*, 2016; 10(16): 4249-4256.
<https://doi.org/10.1049/iet-gtd.2016.0796>
- [10] Shouxiang Wang, Xingyou Zhang, Lei Wu, *et al.*, "New metrics for assessing the performance of multi-microgrid systems in stand-alone mode," *International Journal of Electrical Power & Energy Systems*, 2018; 98: 382-388.
<https://doi.org/10.1016/j.ijepes.2017.12.002>
- [11] Ali Abdali, Reza Noroozian, Kazem Mazlumi, "Simultaneous control and protection schemes for DC multi microgrids systems," *International Journal of Electrical Power & Energy Systems*, 2019; 104: 230-245.
<https://doi.org/10.1016/j.ijepes.2018.06.054>
- [12] Yahya Naderi, Seyed Hossein Hosseini, Saeid Ghassem Zadeh, *et al.*, "An optimized direct control method applied to multilevel inverter for microgrid power quality enhancement," *International Journal of Electrical Power & Energy Systems*, 2019; 107: 496-506.
<https://doi.org/10.1016/j.ijepes.2018.12.007>
- [13] A. Ouammi, H. Dagdougui, L. Dessaint, *et al.*, "Coordinated Model Predictive-Based Power Flows Control in a Cooperative Network of Smart Microgrids," *IEEE Transactions on Smart Grid*, 2015; 6(5): 2233-2244.
<https://doi.org/10.1109/TSG.2015.2396294>
- [14] A. K. Marvasti, Y. Fu, S. DorMohammadi, *et al.*, "Optimal Operation of Active Distribution Grids: A System of Systems Framework," *IEEE Transactions on Smart Grid*, 2014; 5(3): 1228-1237.
<https://doi.org/10.1109/TSG.2013.2282867>
- [15] J. Lee, J. Guo, J. K. Choi, M. Zukerman, "Distributed Energy Trading in Microgrids: A Game-Theoretic Model and Its Equilibrium Analysis," *IEEE Transactions on Industrial Electronics*, 2015; 62(6): 3524-3533.
<https://doi.org/10.1109/TIE.2014.2387340>
- [16] S. Park, J. Lee, G. Hwang and J. K. Choi, "Event-Driven Energy Trading System in Microgrids: Aperiodic Market Model Analysis With a Game Theoretic Approach," *IEEE Access*, 2017; 5: 26291-26302.
<https://doi.org/10.1109/ACCESS.2017.2766233>
- [17] S. Park, J. Lee, S. Bae, *et al.*, "Contribution-Based Energy-Trading Mechanism in Microgrids for Future Smart Grid: A Game Theoretic Approach." *IEEE Transactions on Industrial Electronics*, 63 (7): 4255-4265, 2016.
<https://doi.org/10.1109/TIE.2016.2532842>
- [18] A. M. Jadhav and N. R. Patne, "Priority-Based Energy Scheduling in a Smart Distributed Network With Multiple Microgrids," *IEEE Transactions on Industrial Informatics*,

- 2017; 13(6): 3134-3143.
<https://doi.org/10.1109/TII.2017.2671923>
- [19] N. A. Funde, M. M. Dhabu, P. S. Deshpande, *et al.*, "SF-OEAP: Starvation-Free Optimal Energy Allocation Policy in a Smart Distributed Multimicrogrid System," *IEEE Transactions on Industrial Informatics*, 2018; 14(11): 4873-4883.
<https://doi.org/10.1109/TII.2018.2810816>
- [20] X. Hu and T. Liu, "Co-optimisation for distribution networks with multi-microgrids based on a two-stage optimisation model with dynamic electricity pricing," *IET Generation, Transmission & Distribution*, 2017; 11(9): 2251-2259.
<https://doi.org/10.1049/iet-gtd.2016.1602>
- [21] M. Khalid and A. V. Savkin, "Closure to discussion on "A method for short-term wind power prediction with multiple observation points"," *IEEE Transactions on Power Systems*, 2013; 28(2): 1898-1899.
<https://doi.org/10.1109/TPWRS.2013.2255351>
- [22] C. Wan, J. Lin, Y. Song, *et al.*, "Probabilistic Forecasting of Photovoltaic Generation: An Efficient Statistical Approach," *IEEE Transactions on Power Systems*, 2017; 32(3): 2471-2472.
<https://doi.org/10.1109/TPWRS.2016.2608740>
- [23] Nanfang Yang, Babak Nahid-Mobarakeh, Fei Gao, *et al.*, "Modeling and stability analysis of multi-time scale DC microgrid," *Electric Power Systems Research*, 2016; 140: 906-916.
<https://doi.org/10.1016/j.epsr.2016.04.014>
- [24] Md Alamgir Hossain, Hemanshu Roy Pota, Md Jahangir Hossain, "Evolution of microgrids with converter-interfaced generations: Challenges and opportunities," *International Journal of Electrical Power & Energy Systems*, 2019; 109: 160-186.
<https://doi.org/10.1016/j.ijepes.2019.01.038>
- [25] Y. Xia, W. Wei, M. Yu, *et al.*, "Decentralized Multi-Time Scale Power Control for a Hybrid AC/DC Microgrid With Multiple Subgrids," *IEEE Transactions on Power Electronics*, 2018; 33(5): 4061-4072.
<https://doi.org/10.1109/TPEL.2017.2721102>
- [26] Guibin Zou, Yuwei Ma, Jingjing Yang, *et al.*, "Multi-time scale optimal dispatch in ADN based on MILP," *International Journal of Electrical Power & Energy Systems*, 2018; 102: 393-400.
<https://doi.org/10.1016/j.ijepes.2018.04.036>
- [27] X. Lei, T. Huang, Y. Yang, *et al.*, "A Bi-layer Multi-Time Coordination Method for Optimal Generation and Reserve Schedule and Dispatch of a Grid-Connected Microgrid," *IEEE Access*, Early Access.
- [28] H. Xin, R. Zhao, L. Zhang, *et al.*, "A Decentralized Hierarchical Control Structure and Self-Optimizing Control Strategy for F-P Type DGs in Islanded Microgrids," *IEEE Transactions on Smart Grid*, 2016; 7(1): 3-5.
<https://doi.org/10.1109/TSG.2015.2473096>
- [29] Gibran Agundis-Tinajero, Juan Segundo-Ramírez, Nancy Visairo-Cruz, "Power flow modeling of islanded AC microgrids with hierarchical control," *International Journal of Electrical Power & Energy Systems*, 2019; 105: 28-36.
<https://doi.org/10.1016/j.ijepes.2018.08.002>
- [30] Zhanqiang Zhang, Chunxia Dou, Dong Yue, *et al.*, "Neighbor-prediction-based networked hierarchical control in islanded microgrids," *International Journal of Electrical Power & Energy Systems*, 2019; 104: 734-743.
<https://doi.org/10.1016/j.ijepes.2018.07.057>
- [31] Yang Li, Zhen Yang, Guoqing Li, *et al.*, "Optimal scheduling of isolated microgrid with an electric vehicle battery swapping station in multi-stakeholder scenarios: A bi-level programming approach via real-time pricing," *Applied Energy*, 2018; 232: 54-68.
<https://doi.org/10.1016/j.apenergy.2018.09.211>

Received on 06-11-2022

Accepted on 15-12-2022

Published on 20-12-2022

DOI: <https://doi.org/10.31875/2410-2199.2022.09.10>© 2022 Wang *et al.*; Zeal Press.

This is an open access article licensed under the terms of the Creative Commons Attribution License

(<http://creativecommons.org/licenses/by/4.0/>) which permits unrestricted use, distribution and reproduction in any medium, provided the work is properly cited.